ESTIMATING SOIL WATER DIFFUSIVITY ACROSS A RAINFED OLIVE ORCHARD USING MEASUREMENTS FROM A SENSOR NETWORK

A.J. Espejo-Pérez[1*], J.V. Giráldez[1,2], K. Vanderlinden[3], A. Pedrera[3], G. Martínez[1,4], M. Morón[3] and E.V. Taguas[5]

[1]University of Cordoba, Dpt. of Agronomy, Edif. Leonardo Da Vinci, Ctra. Madrid km 396, 14071 Cordoba. e-mail: g82espea@uco.es
[2]Institute of Sustainable Agriculture. CSIC. Alameda del Obispo s/n, 14004 Córdoba, Spain. e-mail: ag1gicej@uco.es.
[3]IFAPA, Centro Las Torres-Tomejil, Ctra. Sevilla-Cazalla km 12.2, 41200 Alcalá del Río, Sevilla, Spain. e-mail: karl.vanderlinden@juntadeandalucia.es, aura.pedrera.ext@juntadeandalucia.es, manuel.moron.garciabaquero@juntadeandalucia.es.
[4]Environmental Microbial and Food Safety Lab, U.S. Department of Agriculture, Agriculture Research Center, Beltsville, Maryland, USA. e-mail: z42magag@uco.es
[5]University of Cordoba, Dpt. of Rural Engineering. Edif. Leonardo Da Vinci, Ctra. Madrid km 396, 14071 Cordoba. e-mail: evtaguas@uco.es

ABSTRACT. The assessment of soil hydraulic properties is essential for the description of water, energy and chemical transfer processes. However, their measurements are not straight-forward and require considerable effort. A simple methodology to estimate water transmission parameters is presented in this work using data from a network of capacitance probes installed in a rainfed olive orchard. The method is based on the analysis of measured soil moisture profiles during drying periods of the hydrological year 2011-12, using the Boltzmann transform of space and time coordinates. Soil water diffusivity, D(θ), and its variation were successfully estimated within the catchment with the proposed method. This parameter directly influenced the soil moisture dynamics and its spatial variation elucidated differences between areas under the tree canopies (UC) and inter row (IR) areas.

RESUMEN. La determinación de las propiedades hidráulicas del suelo es indispensable para la descripción de los procesos de transferencia de agua, contaminantes y energía. Sin embargo, su obtención no es inmediata y requiere de un esfuerzo sustancial en tiempo y recursos. En este artículo se recurre a un método basado en la transformación de Boltzmann para las coordenadas de profundidad y tiempo, para estimar unos parámetros hidráulicos del suelo a partir de medidas de la humedad con una red de sensores en una cuenca de olivar de secano. Se evaluó la difusividad del agua en el suelo y su variación espacial dentro de la cuenca diferenciando entre las zonas bajo copa de árboles y entre hileras de árboles.

1.- Introduction

A large area of the Mediterranean basin is dedicated to rainfed olive cropping. Being a profitable crop with a great resistance to hard environmental conditions, the future of the crop and the population based on its culture depend on the adoption of rational soil and water conservation management practices (McNeill, 2002). The knowledge of soil water processes is essential to formulate these practices.

Labour-intensive daily soil water content monitoring schemes are often adopted in such studies (*e.g.* Jackson, 1973; Pan et al., 2012). Sensor networks alleviate the work load and offer the possibility of monitoring soil moisture with larger spatial densities and higher frequencies (*e.g.* Mittelbach et al., 2011; Fares et al., 2013).

However, an improved characterization and quantification of soil hydraulic parameters is required for a correct description of vadose zone processes, so that the high-resolution soil water measurement can be optimally used (Vereecken et al., 2008; Martínez et al., 2013).

This report presents a simple method to estimate soil water transmission properties from moisture measurements made during 2011-2012 period. We illustrate how the method can be used to improve our understanding of soil water processes and the influence of the olive tree canopy on water and thermal regimes.

2.- Material and methods

2.1.- Soil water monitoring with a sensor network

The moisture profiles were measured in an experimental catchment located in Setenil de las Bodegas (Cádiz), 36º 52.2' N, 5º 7.8' W, with an average elevation of 776 m-amsl. The soil is dedicated to olive groves (Taguas *et al*., 2009). The trees were 18 years old and were planted on a 6 × 6-m grid. The projected average canopy area was 20 m^2, with a canopy height and diameter of 2.9 and 3.7 m, respectively. The soil overlies a shallow hardened bedrock consisting of calcarenites, limiting soil depth from 0.05 to 1.20 m. The soil subgroup is an intergrade between Lithic and Typic Rhodoxeralf (García del Barrio et al., 1971; Soil Survey Staff, 1999, pp. 269-270). Soil texture was classified as sandy loam. Mean topsoil bulk density at UC and IR locations was 1.59 and 1.74 Mg m^{-3}, respectively. The soil water sensor network consisted

of 11 locations with a total of 108 sensors (10 5TE and 98 10HS; Decagon Devices, Pullman, WA). Both sensors measures volumetric water content via the dielectric constant of the soil using capacitance technology. Besides moisture, the 5TE sensor measures temperature and electrical conductivity. Sensors were placed at a distance of 0.75 m from the tree trunk towards south-east in the UC areas and in the north-east direction in the adjacent IR area. They were installed horizontally at depths of 0.05, 0.15, 0.25, 0.35 and 0.45 m where possible. The time measurement interval was 5 min. Gravimetric moisture content was periodically measured near the sensors and used for their calibration.

Rainfall was measured in the catchment using an automatic rain gauge. Fig. 1 shows the monthly rainfall at the site during three hydrological years, and daily maximum and minimum temperatures at UC and IR locations during 2011-2012.

2.2.- Estimation of soil water diffusivity using Boltzmann coordinates

Due to the frequent and long periods between rainfall events during 2011-2012, a preliminary inspection of the data analysis detected a predominantly diffusive pattern of the moisture content profiles (Suleiman and Ritchie, 2003). Under such circumstances the hydraulic diffusivity parameter, D, could be estimated using the Bruce and Klute (1956) method (Eq. 1, 2, and 3). When the gravitational gradients are negligible, as compared to the suction gradients, the Richards equation can be reduced to the simple version valid for a horizontal diffusion in a semi-infinite unsaturated porous medium,

$$\frac{\partial\theta}{\partial t}=\frac{\partial}{\partial z}\left(k\frac{\partial\psi_m}{\partial z}\right)\equiv\frac{\partial}{\partial z}\left(D\frac{\partial\theta}{\partial z}\right) \qquad (1)$$

where θ is the volumetric water content, t the time, and z the space coordinate. The hydraulic conductivity is k and the matric component of soil water potential is ψ_m. The initial and boundary conditions of the drying process are:

$$\begin{aligned}&\theta=\theta_2 \quad t=0 \quad z\geq 0\\ &\theta=\theta_1 \quad t\geq 0 \quad z=0\\ &\theta=\theta_2 \quad t\geq 0 \quad z\to\infty\end{aligned} \qquad (2)$$

with θ_2 as the initial, wet, and θ_1 the final, dry, moisture content. Adopting the Boltzmann transformation, $\eta = zt^{-1/2}$, Eq. (1) becomes an ordinary differential equation, from which the diffusivity can be estimated as,

$$D(\theta)=-\frac{1}{2}\left(\frac{d\eta}{d\theta'}\right)_\theta\int_{\theta_1}^{\theta}\eta(\theta')\,d\theta' \qquad (3)$$

The boundary conditions shown in Eq. (2) with the new Boltzmann coordinate become then

$$\begin{aligned}&\theta=\theta_2 \quad \eta\to\infty\\ &\theta=\theta_1 \quad \eta=0\end{aligned} \qquad (4)$$

The Philip (1957) sorptivity, S, is obtained as the integral of Eq. (3). Several methods have been proposed for the numerical resolution of Eq. (3) (*e.g.* Kirkham and Powers, 1972 § 6.G.2, Warrick, 2003 § 4.4). Initially a least squares spline curve, (Kimball, 1976), was chosen to keep the information of all field data. Nevertheless, an exponential fit with two constants was adopted given the exponential trend observed in the data for simplicity and uniformity purposes

$$\theta=\theta_2\left[1-\exp(-a\eta)\right], \qquad (5)$$

with a a fitting parameter. The Boltzmann coordinate becomes then

$$\eta=-\frac{1}{a}ln\left(1-\frac{\theta}{\theta_2}\right). \qquad (6)$$

The sorptivity is, therefore

$$S(\theta_0,\theta)=\int_{\theta_1}^{\theta}\eta\,d\theta=-\frac{1}{a}\ln\left[\frac{\theta_2^{(\theta-\theta_1)}(\theta_2-\theta)^{(\theta_2-\theta)}}{(\theta_2-\theta_1)^{(\theta_2-\theta_1)}}\right] \qquad (7)$$

and the diffusivity,

$$D(\theta)=-\frac{S(\theta_1,\theta)}{2a(\theta_2-\theta)} \qquad (8)$$

The value of the diffusivity D(θ) was estimated at each of the 11 sites, both for UC and IR. The method requires soil moisture measurements for a complete and continuous drying period Hence, the drying period considered was from 20 May 2012 to 19 September 2012. Only moisture values for which the difference with the preceding measurement was > 0.0008 m^3m^{-3} were retained for the analysis.

3.- Results and discussion

The annual precipitation during the hydrological year 2011-12 at the site was 315 mm (Fig. 1). During the rainy season, December to March, the cumulative rain depth was 28 mm. During the summer season the maximum value of soil temperature for IR was 6-8 ºC greater than UC, similar to air temperature. The spatial variation of soil temperature was higher when the soil dried, indicating the buffering effect of moisture.

The sensors efficiently recorded changes in soil moisture as a result of rainfall and the subsequent loss of moisture during inter-rain periods. The IR locations were wetter than UC. Fig. 2 shows that some rainfall events

(*e.g.* 5 mm h^{-1} in May or 20 mm h^{-1} in September) were not detected at UC locations. Often, these rainfall events were associated with high wind speeds. For example, during the September shower the wind speed increased from 3.9 two hours before the rain to 9.9 m s^{-1} during rainfall.

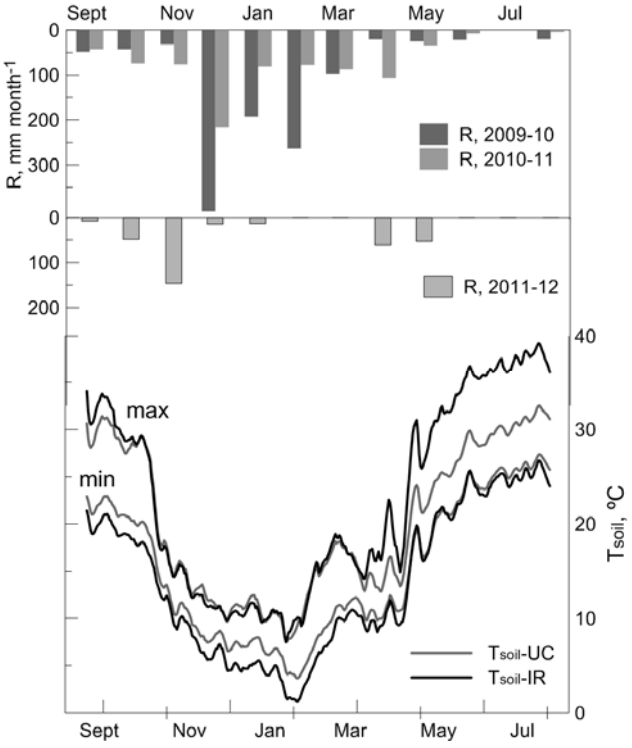

Fig. 1. Monthly rainfall at the Setenil de las Bodegas site during the hydrological years 2009-10, 2010-11, and 2011- 12, and daily minimum and maximum soil temperature at the depth of .05 m during the hydrological year 2011-12, at UC and IR locations

The lower moisture at UC contrasts with the observations of other authors for different tree species with larger canopies and volume of stored water under the canopy (*e.g.* Liang et al. 2011). In a pinyon-juniper woodland in the South West of the United States, Lebron et al. (2007) found that soil was wetter near the trunk, driest at 1.1 m from the trunk, to increase again to a maximum value at 2.2 m near the edge of the canopy. In the case of olive trees, Gómez et al. (2002) found that canopies were fully saturated during exceptionally intense rainfall events. In their study they detected that 60% of the stemflow infiltrated into a circular area with radius of 0.2 m around the trunk. The lower water storage measured here could be attributed to the reduced magnitude of rain events that usually did not saturate the canopy and the location of UC sites at the driest distance to the trunk according to Lebron et al. (2007). The mean rainfall depth per event considering that the time separation between two consecutive events was 6 hours was 9.6 mm, and the minimum and maximum values were 0.9 and 29.3 mm. In a 56% of the case the rainfall depth was lower than average value.

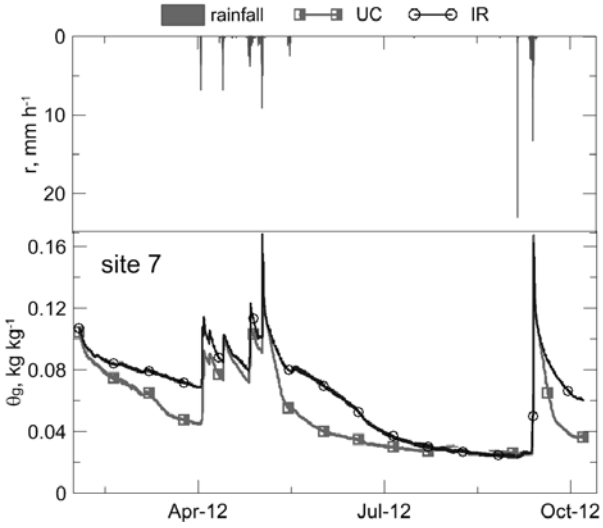

Fig. 2. Evolution of the mean gravimetric moisture of the profile at UC and IR locations of site 7. Hourly rain intensities are shown in the upper graph

Relevant differences were found in the wetting and drying rates. The response to rainfall at UC locations usually lagged behind 6 hours as compared to IR (Fig. 3). During this rainfall event the total moisture increment in the top 0.05 m layer at UC and IR locations was 0.04 and 0.07 kg kg^{-1}, respectively.

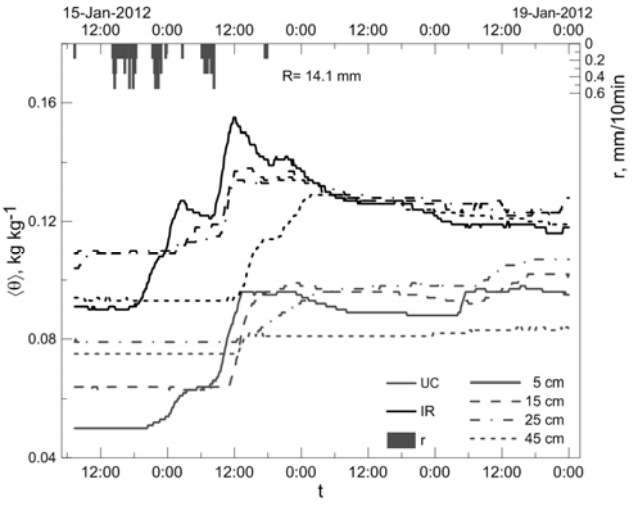

Fig. 3. Time evolution of the spatial mean gravimetric moisture, during and after a low intensity rain event

Fig. 4 shows moisture profiles at consecutive times after a rainfall event of 77 mm for UC and IR locations at site 7. The drying process lasted 11 days. Soil moisture decreased rapidly down to the depth of 0.15 m at UC during the first day after the rain. This initial and quick response was also appreciated in the temporal evolution of the mean moisture profile (Fig. 2). Although soil

processes are slower than atmospheric processes, the transitions are also abrupt, and their observation requires therefore a short temporal monitoring resolution. When the evaporative demand was low, as occurred during the winter months, the drying of the surface and subjacent layers was slower. In general, the measurements showed a more pronounced curvature of the moisture profiles, especially for UC, when there was enough water stored in the soil profile. Similar patterns were identified when the evaporative demand was very high. These results illustrate the contribution of capillary forces to supply water from deeper layers to the surface soil in order to satisfy the atmospheric demand.

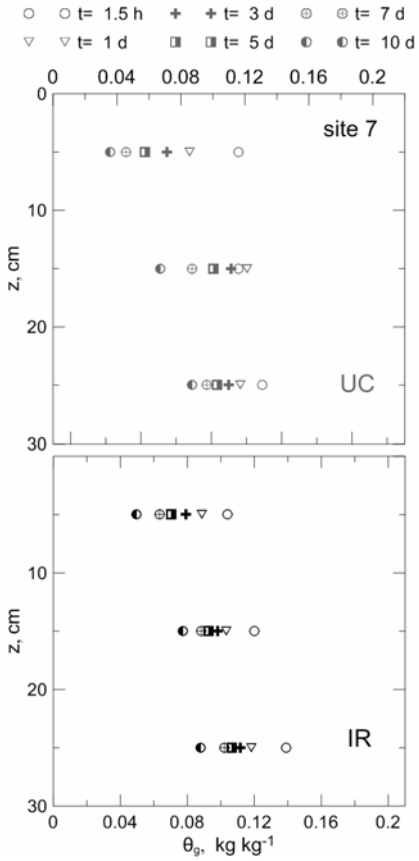

Fig. 4. Soil moisture profiles for site 7 during a short drying period from 8-18 May 2012. Moisture is expressed in gravimetric units

The fit of Eq. (5) to the measured data for site 5 is shown in Fig. 5, considering separately UC and IR locations. The fitted θ_2 and a values, and associated coefficients of determination, are given in table 1 and 2 for IR and UC locations, respectively.

A Tukey test (Croarkin and Tobias, 2003) showed significant differences between IR and UC for both, θ_2 and a. The acceptance probability was 0.023 and 0.002 for θ_2 and a, respectively. The standard deviations of θ_2 and a were higher at the IR locations as compared to UC.

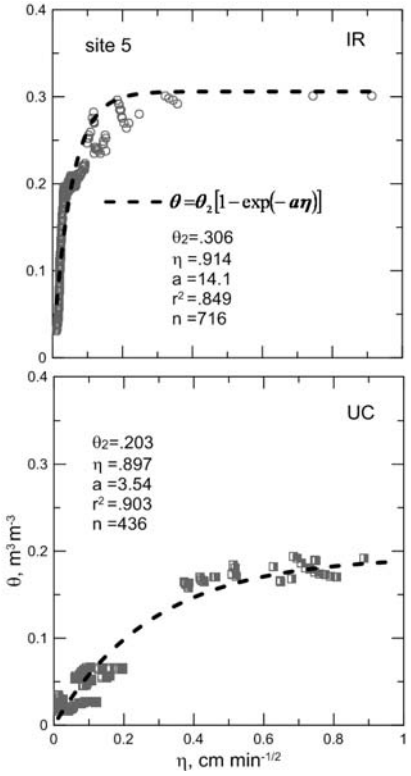

Fig. 5. Soil moisture profiles for site 5: IR (top) and UC (bottom), as a function of the Botzmann coordinate

Values of θ_2 were lower UC at all sites, even though the porosity as estimated form the bulk density was higher in UC. Antecedent rainfall events were small and supplied less water to the soil UC as a result of canopy interception, as shown in Fig. 1 and 2. Antecedent rainfall was 27.4 mm on 5 May and 2.56 on 20 May, distributed during 18 and 5 hours, respectively.

Table 1. Parameter values for the exponential fit to the observed values of the transformed soil water content for IR, and summary of statistical analysis of the exponential fit parameters

site	θ_2	a	r^2	n
	$m^3\ m^{-3}$	$cm^{-1}min^{1/2}$		
05	.306	19.1	.849	766
07	.252	5.44	.845	346
09	.256	7.06	.774	341
19	.291	12.0	.909	947
21	.224	11.0	.824	989
23	.271	15.0	.809	314
25	.325	14.5	.933	1846
34	.226	15.8	.931	434
36	.326	25.6	.852	1503
38	.285	17.2	.842	1231
42	.349	9.90	.932	817
mean	.283	13.7		
s	.042	5.70		
K-S stat. †	.117	.115		
Critical K-S stat ‡	.391	.391		

† Kolmogorov-Smirnov statistic for the Gaussian probability function fit; ‡ Significance level, *α=.05; n:* number of data used

Table 2. Parameters values for the exponential fit to the observed values of the transformed soil water content for UC, and summary of statistical analysis of the exponential fit parameters

site	θ_2	a	r^2	n
	$m^3 m^{-3}$	$cm^{-1}min^{1/2}$		
05	.203	3.54	.903	436
07	.255	3.64	.768	314
09	.320	2.45	.864	259
19	.239	8.98	.879	1217
21	.220	6.19	.725	405
23	.273	11.7	.887	781
25	.238	14.3	.869	789
34	.208	3.46	.945	343
36	.201	8.19	.573	159
38	.239	4.44	.918	631
42	.268	4.18	.935	411
mean	.242	6.35		
s	.036	3.74		
K-S stat. †	.171	.265		
Critical K-S stat ‡	.391	.391		

The estimated hydraulic diffusivity function for the site 7 is shown in Fig. 6. The shape of the curves agrees with that reported by Evangelides et al. (2010) using an empirical multivariable complex function for the description of the transformed moisture profile. In all cases the diffusivity acquired an exponential dependency on the soil water content above 0.15 m^3 m^{-3} becoming infinite at θ_2. Even though both curves were similar for the sites, diffusivity was higher at the UC locations.

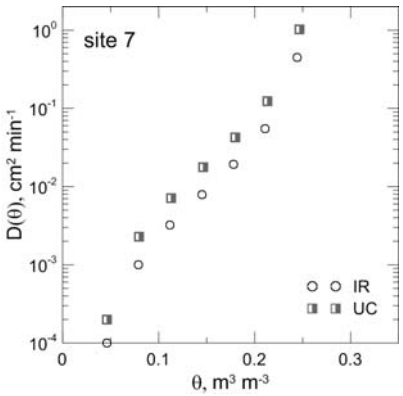

Fig. 6. Estimated soil water diffusivity function for site 7

The higher values of diffusivity at UC locations could be attributed to the greater organic matter content due to the falling leaves and dead roots and protecting role of the canopy retarding organic matter decay. The beneficial effect of soil organic matter on structure could favor higher transmission rates for water.

The differences in diffusivity values between IR and UC were larger for wetter conditions, and reached an average of 0.88 cm^2 min^{-1} with a maximum reaching 2.00. The higher *D(θ)* values for UC may explain the faster decrease of moisture at these locations as compared to IR.

Sites 7 and 9 showed the highest values of *D(θ)* for IR and UC. These sites were located in areas of the catchment with a shallow soil profile and protruding rock fragments. The *D(θ)* near saturation had a maximum value of 4.08 cm^2 min^{-1}. In general, the estimated values were within the acceptable range but were slightly lower than the values reported by Wang et al. (2004), especially for IR areas. The results revealed spatial patterns in the the catchment, which we will further explore. For example site 36 showed very low diffusivity values which can be attributed to frequent farm machinery traffic.

The normalized values of moisture contents and Boltzmann coordinates were calculated for each site to test the method. Fig. 7 shows the normalized data for each site considering separately UC and IR locations. All data collapsed to a curve with the shape a Gaussian probability distribution function with an initial increase until values of 0.80 for the normalized moisture in IR locations and 0.90 for UC.

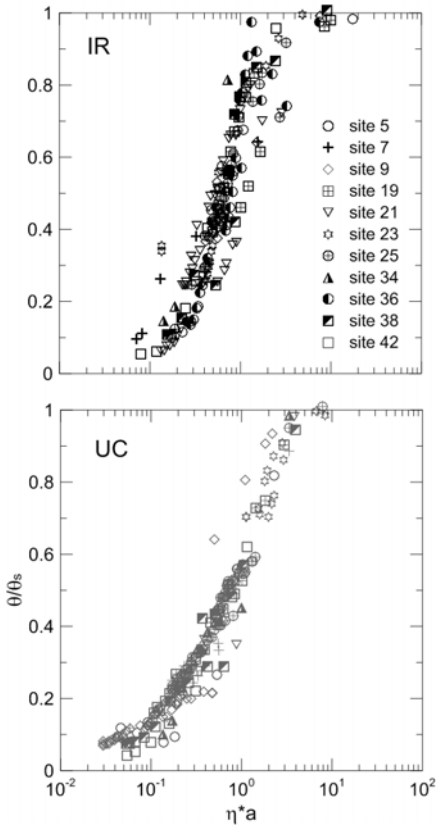

Fig. 7. Relation between normalized values of moisture and η using θ_2 and *a* values of each point, for IR (top) and UC (bottom)

A more rigorous parameter identification method can be applied, but the simple approach adopted here gives good results.

4.- Conclusions

This work showed that traditional laboratory methods for characterizing soil physical properties can be extended to field data using information obtained from soil moisture sensor networks, avoiding the difficulties of early soil water sampling processes (*e.g.* Jackson, 1963). More specifically, this work provides a simple method to estimate soil water diffusivity from soil moisture sensor data.

Steadily lower water contents were found at UC locations as compared to the IR areas, although temporal soil water dynamics were similar for both locations.

The soil drying process following rain water infiltration could be represented as an exponentially decreasing function of time using the traditional Boltzmann transformation for all locations and inter-rain periods. A faster decrease of the moisture profile was observed in UC than IR areas. The lower water content at UC areas could be explained by the higher soil water diffusivity during dry periods in UC.

The method described will be used for further research to describe soil water dynamics during other periods of the year and to compare the results with laboratory-measured soil physical properties.

Acknowledgements. This work was supported by the MINECO and the Consejería de Innovación Ciencia y Empleo de la Junta de Andalucía through the Research Projects AGL2009-12936-C03-03, AGL2012-40128-C03-03 and AGR 1782. The senior author acknowledges a Predoctoral Fellowship P-09 by the Junta de Andalucía through the latter Research Project. We appreciate also the assistance of J. García and M.A. Ayala of IFAPA Las Torres-Tomejil with the field and laboratory work.

5.- References

Bruce, R.R., and A. Klute, 1956. The measurement of soil moisture diffusivity. *Soil Sci. Am. Proc. 20*, 458-462.

Croarkin, C., and P. Tobias, 2003. *NIST/SEMATECH e-Handbook of Statistical Methods*, http://www.itl.nist.gov/div898/handbook/, [retrieved on 27/5/2012].

Evangelides, C., G. Arampatzis, and C. Tzimopoulos, 2010. Estimation of soil moisture profile and diffusivity using simple laboratory procedures. *Soil Sci.175*, 118-127.

Fares, A., M. Temimi, K. Morgan, and T.J. Kelleners, 2013. In-situ and remote soil moisture sensing technologies for vadose zone hydrology. *Vadose Zone J*., doi:10.2136/vzj2013.03.0058

García del Barrio, I., L. Malvárez, J.I. González, 1971. *Mapas provinciales de suelos. Cádiz*. Ministerio de Agricultura. Madrid.

Gómez, J.A., K. Vanderlinden, J.V. Giráldez, and E. Fereres, 2002. Rainfall concentration under olive trees. *Agric. Water Manag. 55*, 53-70.

Jackson, R.D., 1963. Porosity and soil water diffusivity relations. *Soil Sci. Soc. Am. Proceed. 27* (2), 123-126.

Jackson, R.D., 1973. Diurnal changes in soil waster content during drying, in Bruce, R.R., K.W. Flach, and H.M. Taylor eds. *Field soil water regime*, Soil Sci. Soc. Am. Spec. Publ. No 5. Soil Sci. Soc. Am. Madison, WI, Chap. 3.

Kimball, B.A., 1976. Smoothing data with cubic splines. *Agron. J. 68*, 126-129.

Kirkham, D., and W.L. Powers, 1972. *Advanced soil physics*. J. Wiley, New York.

Lebron, I., M.D. Madsen, D.G. Chandler, D.A. Robinson, O. Wendroth, and J. Belnap, 2007. Ecohydrological controls on soil moisture and hydraulic conductivity within a pinyon-juniper Woodland. *Water Resour. Res. 43*, doi: 10.1029/2006WR005398.

Liang, W.L., K. Kosugi, and T. Mizuyama, 2011. Soil water dynamics around a tree on a hillslope with or without rainwater supplied by stemflow. *Water Resour. Res. 47*, W02541, doi:10.1029/2010WR009856.

Martínez, G., Y.A. Pachepsky, and H. Vereecken, 2013. Temporal stability of soil water content as affected by climate and soil hydraulic properties: a simulation study. *Hydrol. Proc.* doi: 10.1002/hyp.9737.

McNeill, J.R., 2002. *The mountains of the Mediterranean world: an environmental history*. Cambridge Univ. Press, Cambridge.

Mittelbach, H., F. Casini, I. Lehner, A.J. Teuling, and S.I. Seneviratne, 2011. Soil moisture monitoring for climate research: Evaluation of a low cost sensor in the framework of the Swiss Soil Moisture Experiment (SwissSMEX) campaign. *J. Geophys. Res. 116*, D05111, doi:10.1029/2010JD014907.

Pan, F., Y. Pachepsky, Yakov, D. Jacques, A. Guber, A. Hill, and L. Robert, 2012. Data Assimilation with Soil Water Content Sensors and Pedotransfer Functions in Soil Water Flow Modelling. *Soil Sci. Soc. Am. J. 276*, 829–844, doi: 10.2136/sssaj2011.0090.

Philip, J.R., 1957. The theory of infiltration: 4. Sorptivity and algebraic infiltration equation. *Soil Sci. 84*, 257-264.

Soil Survey Staff, 1999. *Soil Taxonomy*. 2nd. ed. USDA Agr. Hdbk. No. 436. NRCS. Washington.

Suleiman, A.A., and J.T. Ritchie, 2003. Modeling soil water redistribution during second-stage evaporation. *Soil Sci. Soc. Am. J. 67*, 377–386, doi: 10.2136/sssaj2003.3770.

Taguas E.V., J.L. Ayuso, A. Peña, Y. Yuan, and R. Pérez, 2009. Evaluating and modelling the hydrological and erosive behaviour of an olive orchard microcatchment under no-tillage with bare soil in Spain. *Earth Surf. Process. Landforms, 34*, 738–751, DOI: 10.1002/esp

Vereecken, H., J.A. Huisman, H. Bogena, J. Vanderborght, J.A. Vrugt, and J.W. Hopmans, 2008. On the value of soil moisture measurements in vadose zone hydrology: A review. *Water Resour. Res., 44*: W00D06, doi:10.1029/2008WR006829.

Wang, Q., M. Shao, and R. Horton, 2004. A simple method for estimating water diffusivity of unsaturated soils. *Soil Sci. Soc. Am. J. 68*, 713-718.

Warrick, A.W, 2003. *Soil water dynamics*. Oxford Univ. Press.